Journal of Applied Electrochemistry (2007) 37:187–194
DOI 10.1007/s10800-006-9256-2

An electrochemical study of corrosive wear of phosphate grinding mill

D. TAO[1,*], G.L. CHEN[1] and B.K. PAREKH[2]
[1]*Department of Mining Engineering, University of Kentucky, 234 MMRB, Lexington, KY 40506, USA*
[2]*Center for Applied Energy Research, University of Kentucky, Lexington, KY 40514, USA*
*(*author for correspondence, tel.: + 1-859-257-2953, fax: + 1-859-323-1962, E-mail: dtao@engr.uky.edu)*

Received 9 August 2005; accepted in revised form 23 March 2006

Key words: abrasive wear, ball mill grinding, cathodic protection, corrosive wear, surface characterization

Abstract

The corrosion of metallic grinding media and mill liner is a very significant problem, particularly under acidic conditions as encountered in the Florida phosphate fertilizer industry. Approximately half of grinding media wear results from corrosion or oxidation dissolution of metal surfaces. An electrochemical cathodic protection process based on impressed current was investigated to reduce wear rates of metals by reducing their electrochemical potentials with excess electrons. The polarization potential and current density required to minimize corrosion were determined using a specially designed ball mill whose electrochemical potential can be controlled. Phosphate grinding tests under controlled electrochemical conditions show that the corrosive wear can be reduced by more than 90% and the overall wear rate by more than 50%. SEM, EDS, and XRD studies were conducted to understand process fundamentals.

1. Introduction

The United States is the largest phosphate rock producer in the world. About 30% of the world production was produced by the United States [1]. The State of Florida accounts for approximately 80% of U.S. phosphate production [2]. Approximately 95% of produced phosphate is consumed by fertilizer plants where phosphorus, together with nitrogen and potassium, is used to make plant fertilizers. Phosphate is also an important component of tooth paste, detergents, food, etc.

Grinding mills are commonly used in the Florida phosphate industry to reduce particle size. The corrosion of metallic grinding media and mill liner is a very serious problem, particularly under acidic conditions as encountered in the Florida phosphate fertilizer industry (pH 2–4). At acidic pH, protective passivation films of metal oxides and/or hydroxides do not exist on the surface of balls and liners, exposing fresh metal surface that is more susceptible to corrosion. It is known that the corrosive wear of grinding mill leads to an increase in operating cost and plant downtime, a loss of process efficiency, and product contamination. The direct operating costs in grinding are mainly the energy consumed and the metal lost through wear and corrosion [3, 4]. An effective protection of grinding mills from corrosion will improve the process performance and economics, enhance product quality, and increase the lifetime of mills and grinding media.

Metal corrosion reactions are electrochemical in nature and their reaction rates are controlled by the electrochemical potential at the surface. A reduction in potential with excess electrons (e^-) will depress the anodic dissolution reaction of metal (e.g., $M = M^{2+} + 2e^-$). This can be accomplished by supplying an impressed current to the object to create a negative potential change, referred to as cathodic polarization. Fundamental corrosion analysis indicated that a 0.1 V reduction in potential of the iron or steel electrode can reduce the corrosion rate by more than 99% [5].

2. Experimental

Unlike earlier mill corrosion studies that used devices that merely simulated mill motion, the present study utilized a specially designed ball mill whose electrochemical potential can be controlled under operating conditions [6–9]. The results from this study more closely resemble those expected from the industrial ball mills. The mill was constructed of a stainless steel pipe of 21.6 cm in diameter and 30.5 cm in length with a wall thickness of 0.6 cm, as illustrated in Figure 1. To characterize the weight loss of the ball mill shell or its liner, three coupons made of the material representing the mill shell or liner was installed flush with the interior surface of the mill. These coupons, 1.0 cm in diameter and 2.5 cm in height, were electrically isolated from the

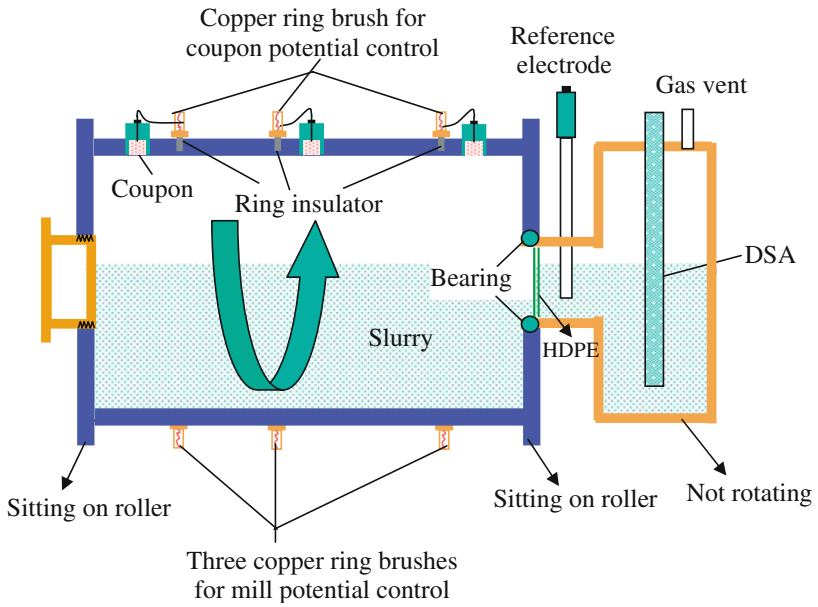

Fig. 1. Schematics of the specially designed mill for grinding tests.

mill. The potential or current of the coupons was controlled via copper brushes riding on the concentric copper ring. The cathodic protection of the ball mill was accomplished using a 0.6 cm in diameter and 30.5 cm in length titanium-indium oxide, dimensionally stable anode (DSA) (acquired from Corrpro Companies Inc., Medina, Ohio) that was located in an anode compartment and isolated from the slurry with a high-density polyethylene (HDPE) membrane to prevent particulates from contaminating the anode. Gases such as oxygen and hydrogen produced at the anode were released from the anode chamber through a vent shown in Figure 1. The potential and current applied to the coupons were controlled using an EG&G PARC, Model 273 potentiostat. An industrial standard calomel electrode (SCE) was used as the reference electrode.

The coupons used to represent the grinding balls and mill shell were made of 1018 carbon steel acquired from McMaster-Carr Supply Company, Cleveland, OH. The compositions of 1018 carbon steel are shown in Table 1. The coupon assembly consisted of the metal coupons in the center and the insulator around it. The total wear of metal was estimated based on the average weight loss of three coupons after grinding.

The phosphate samples and pond water used in this study were acquired from Florida CF Industries, Plant City, Florida. The phosphate sample was thoroughly mixed and wet screened into seven different size fractions for the size distribution analysis and the results are shown in Table 2. It is clear that the particle is quite evenly distributed in all size fractions except the −0.075 mm fraction. The acidic phosphogypsum pond water (pH 1.3) was used as a part of feed water, which is a standard industrial practice. The pond water was mainly comprised of water (~90%), phosphoric acid (< 4%), and sodium potassium fluosilicate (< 1.5%).

Table 1. Compositions of 1018 carbon steel/%

Sample	Fe	C	Mn	P	S
1018 carbon steel	98.53	0.18	0.75	0.04	0.50

Table 2. Phosphate size analysis results

Sample	Wt.%	∑Wt.%
+10 mesh	15.74	15.74
−10 + 20	27.67	43.41
−20 + 40	13.88	57.29
−40 + 60	21.44	78.73
−60 + 100	13.20	91.93
−100 + 200	7.87	99.80
−200	0.20	100.00

The contents of calcium sulfate, fluosilicic acid, sulfuric acid, dissolved metallic impurities, fluorides, and monoammonium phosphate were less than 1%.

Except for the statistically designed factorial experiments described below, the rotation speed of the grinding mill was fixed at 70 rpm which was 75% of the critical speed; the solids percentage was maintained at 64%, which was the same as the industrial practice; the load percentage was kept at 50%. The Box-Behnken Design (BBD) of fractional factorial experiment was conducted to determine effects of individual operating variables and their interactions on the wear rate of grinding ball mills. The fractional factorial design is particularly useful for screening a large number of variables to identify the most significant parameters and optimum condition with a very small number of experiments. Table 3 shows four operating variables examined in this study and their three levels. The wear rate in millimeters penetration per year (MPY) was calculated from Equation (1):

Table 3. Test levels of parameters for BBD

Factor	Units	Coded parameter	Levels		
			−1.0	0.0	+1.0
Solution pH		A	3	7	9
Rotation speed	rpm	B	60	70	80
Crop load	%	C	40	50	60
Solid concentration	%	D	54	64	74

$$\mathrm{MPY} = \frac{2.1W}{DAT}, \tag{1}$$

where W is weight loss in milligrams, D is density in grams per cubic centimeter, A is area in square centimeters, and T is time in hours [5].

3. Results and discussion

3.1. *Polarization study*

The polarization diagram gives a fundamental and quantitative assessment of the change in corrosion rate caused by the cathodic polarization. It was established using a standard three-electrode electrochemical cell controlled by a potentiostat which applied a sweeping potential to the working electrode made of the same metal as the mill or grinding medium (Tao et al. 1994).

Since phosphate grinding takes place in the solution mixture of gypsum pond water and fresh water, polarization studies were carried out in the simulation solution made of gypsum pond water and distilled water. The pH of undiluted gypsum pond water was 1.31. The pond water and NaOH solution were used to make solutions of pH 4.6, 6.8, and 9.2. The potentidynamic cathodic polarization curves of 1018 steel specimen in oxygenated or nitrogenated pond water solutions at these pH's are shown in Figure 2. The pond water solution was bubbled with oxygen or nitrogen for 10 min prior to each experiment. It is obvious that in the oxygenated solution the metal corroded much faster in lower pH solutions than in higher pH solutions, as indicated by the higher current density. At pH 4.6, there was about one decade of Tafel behavior for the hydrogen reduction reaction before the concentration polarization began with a limiting current density of about 20 mA cm^{-2}. As pH increased to 6.8, hydrogen ion activity became much lower, the concentration polarization of reaction (2) began at a much lower current density and the limiting current density decreased to about 1.6 mA cm^{-2}. In the pH 9.2 solution, hydrogen evolution by direct reduction of water (reaction (3)) occurred above the limiting current density for reaction (2). It is clear that the limiting current density was about 12 times greater at pH 4.6 than at pH 6.8. Jones [5] and Stern [10] reached a similar conclusion from the study of effect of solution pH on cathodic polarization of pure iron.

$$2H^+ + 2e^- \rightarrow H_2 \tag{2}$$

$$2H_2O + 2e^- \rightarrow H_2 + 2OH^- \tag{3}$$

Figure 2(b) shows the potentiodynamic cathodic polarization curves of 1018 steel specimen in nitrogenated pond water solutions with pH values of 4.6, 6.8, and 9.2, respectively. Again, the metal corroded much faster in the lower pH solution than in the higher solution, as indicated by the higher current density at lower pH's. The limiting current density was about 35 mA cm^{-2} at pH 4.6, which was about 17 times greater than the limiting current density of 2.04 mA cm^{-2} at pH 6.8.

Comparing Figure 2(a) with Figure 2(b) reveals that the limiting current density was higher in the nitrogenated pond water solution than in the oxygenated pond water solution at the same pH value. This is believed to result from easier passivation of the metal by oxygen in the oxygenated pond water solution.

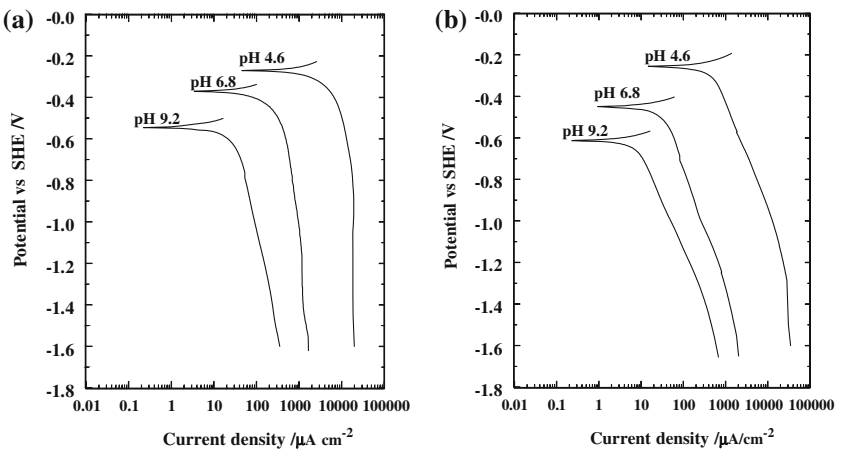

Fig. 2. Potentiodynamic cathodic polarization curve of 1018 carbon steel in (a) oxygenated pond water solutions, and (b) nitrogenated pond water solutions.

3.2. *Effect of polarization potential on corrosion rate*

Anodic polarization represents a driving force for corrosion by the anodic half cell reaction. When solution rest potential measures more positive, the oxidizing (or corrosive) power of the solution increases. To investigate effects of polarized potential on corrosion rate of the ball mill, 3-h grinding tests were conducted using the experimental setup described earlier under controlled electrochemical conditions. The effects of polarization potential on the wear rate of 1018 carbon steel in different solutions were carried out and the results at pH 3.1 are shown in Figure 3. It is obvious that the wear rate decreased with increasing cathodic polarization potential, i.e., making the potential more negative. For example, the wear rate was 19.3 MPY without polarization potential in the pH 3.1 solution, while it was 10.6 MPY at −0.9 V potential in the same solution. Figure 3 clearly indicates that further increasing the cathodic polarization potential from −1.0 to −1.5 V did not improve the ball mill cathodic protection. This suggests that potential of −1.0 V was sufficient to effectively reduce the wear rate of 1018 carbon steel. Similar results were obtained with 1018 carbon steel in pH 6.8 and pH 9.2 solutions and the wear rate was higher in pH 3.1 than in pH 6.8 and pH 9.2 solutions. These experimental data suggested that the total wear rate was reduced by 42% to 46% when a potential of −1.0 V was applied.

The total wear rate of metal determined from the weight loss measurement has three components, which are abrasive wear, corrosive wear and synergistic effect of abrasive and corrosive wear. These wear components can be identified using the approach described elsewhere [11, 12] and the results are also shown in Figure 3. The figure clearly indicates that the corrosive wear of 1018 carbon steel decreased substantially with increasing cathodic polarization potential. The corrosive wear rate was 7.4 MPY without polarization potential in the pH 3.1 solution, but was reduced to 1.0 MPY at −1.0 V polarization potential in the same solution, suggesting that the corrosive wear rate of 1018 carbon steel was reduced by 86% in the pH 3.1 solution. Furthermore, cathodic protection was also effective for reducing the synergistic effect of abrasive wear and corrosive wear as indicated by a 51% reduction in the pH 3.1 solution by applying a −1.0 V polarization potential. But the effect of polarization potential on the abrasive wear was negligible. Pazhianur et al. [8] reported similar results that cathodic protection reduced the material loss in tumbling mills by 30% to 60% when grinding tests were conducted on quartz, pyrite and quartz-pyrite mixtures at pH levels of 4.6, 7.1 and 9.2.

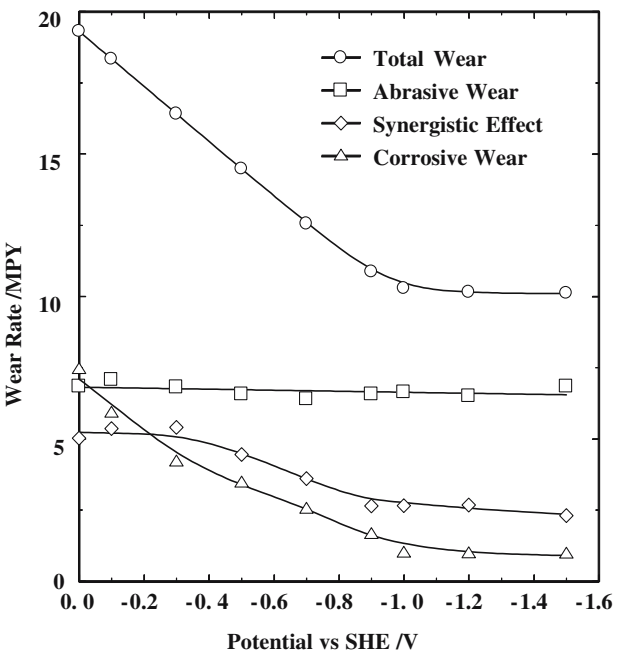

Fig. 3. Effect of polarization potential on corrosion rate of 1018 carbon steel at pH 3.1, rotation speed 70 rpm, crop load 50% and solid percentage 64%.

3.3. *Required current density for effective protection*

The ball mill can be protected from corrosive wear using the impressed current technique which utilizes an external power source to force current out of the DSA, into the electrolyte, and eventually onto the ball mill. The impressed current cathodically polarizes the ball mill and reduces its corrosion rate. The magnitude of impressed current determines the effectiveness of corrosive wear rate reduction. Previous work [13] indicated that the main requirement for effective cathodic protection is that the protective system provides enough current to polarize the structure.

To investigate effects of impressed current density on corrosion rate of the ball mill and grinding media, 3-h grinding tests were conducted under controlled impressed current density that varied at 10, 50, 100, 150, 160, 180, 210, and 250 mA m^{-2}. The change in the total wear, corrosive wear, abrasive wear, and synergistic effect of abrasive wear and corrosive wear were determined for each test and correlated with the applied current density. The difference in the correlation at different pH's indicates the effect of solution pH on the corrosion rate, and possibly corrosion mechanism as well. Thus, the optimum magnitude of impressed current density was readily identified.

The effects of impressed current density on the wear rate of 1018 carbon steel in the pH 3.1 solution are shown in Figure 4. It is obvious that the total wear rate decreased with increasing the impressed current density. For example, the total wear rate was 19.3 MPY without impressed current in the pH 3.1 solution, while it was 10.5 MPY at 210 mA m^{-2} impressed current density in the same solution. Figure 4 clearly reveals that the wear rate maintained a constant value when the impressed current density increased from 210 to 250 mA m^{-2}. This suggests that an impressed current density of 210 mA m^{-2} was sufficient to effectively reduce the wear

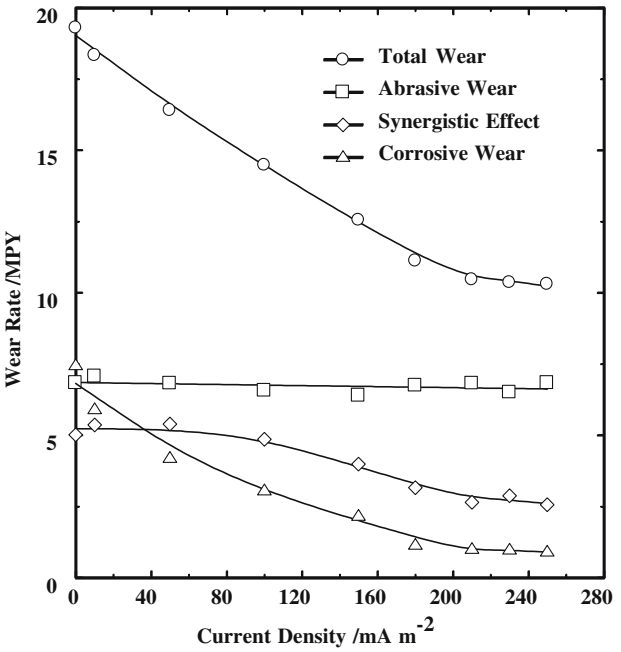

Fig. 4. Effect of impressed current density on corrosion rate of 1018 carbon steel at pH 3.1, rotation speed 70 rpm, crop load 50% and solid percentage 64%.

rate of 1018 carbon steel in the pH 3.1 solution. Figure 4 also suggests that the total wear rate was reduced by 45% when a current density of 210 mA m^{-2} was applied. The required current densities for mill protection are in good agreement with that obtained for the cathodic protection of steel structures by Gartland et al. [14] who concluded that the required current densities for the cathodic protection of steel structures in the North Sea ranged from 50 to 215 mA m^{-2}.

As described earlier, the impressed current density was mainly used to reduce the corrosive wear. The corrosive wear rate was determined using the same approach mentioned earlier and the results are shown in Figure 4. This figure clearly indicates that the corrosive wear of 1018 carbon steel decreased significantly with increasing the impressed current density. The corrosive wear rate was 7.4 MPY without impressed current in the pH 3.1 solution. It was reduced to 1.0 MPY at 210 mA m^{-2} impressed current density in the same solution. In other words, the corrosive wear rate of 1018 carbon steel was reduced by 85%. Cathodic protection was also effective for reducing the synergistic effect of abrasive wear and corrosive wear. For example, the synergistic effect of abrasive wear and corrosive wear was reduced by 47% in the pH 3.1 solution by applying a 210 mA^{-2} current density. But the effect of impressed current density on the abrasive wear was negligible. Similar results were obtained with 1018 carbon steel in pH 6.8 and pH 9.2 solutions. The corrosive wear rate was reduced by 83% in the pH 6.8 solution and 85% in the pH 9.2 solution; the synergistic effect of abrasive wear and corrosive wear was reduced by 40% in the pH 6.8 solution and 54% in the pH 9.2 solution, respectively. These results are consistent with those obtained by the potential control. As described earlier, the total wear rate was reduced by 51% and the corrosive wear rate was reduced by 86% at pH 3.1 by applying −1.0 V polarization potential.

Comparing the above results reveals that the required current density for effective corrosion protection was higher in acidic solutions than in neutral or alkaline solutions. For example, an impressed current density of 210 mA m^{-2} provided sufficient protection from corrosive wear in the pH 3.1 solution, while the required current density was 180 mA m^{-2} in the pH 6.8 solution and 160 mA m^{-2} in the pH 9.2 solution.

3.4. *Corrosion mechanism*

3.4.1. *SEM analysis*

The microstructure of the coupon surfaces corroded at different pH values under different impressed currents were investigated using SEM. Figure 5 shows the SEM images of 1018 carbon steel after it was exposed to phosphate slurry at pH 3.1 for 3 h with and without cathodic protection, respectively. In Figure 5(a), the gouges and scratches on the surface indicate wear due to corrosion and abrasion. The darker spots might be due to the formation of oxides or hydroxides. This figure clearly shows that there are a lot of deep and shallow pits on the surface, suggesting that pitting corrosion was the main corrosion mechanism. Pitting corrosion was caused by localized attacks in an otherwise resistant surface. The rate of corrosion was greater in some areas than others. Pitting corrosion was caused by the presence of phosphoric acid, fluosilicic acid, and sulfuric acid that managed to pass through the passive film and initiate corrosion, resulting in rupture of the passive film. Figure 5(b) shows the SEM image obtained when a polarization potential of −1.0 V was applied. This image shows fewer dark spots, indicating a reduction of corrosion on the surface. Similar images were obtained with 1018 carbon steel in the pH 6.8 and 9.2 solutions.

3.4.2. *EDS analysis*

To produce the coupon sample for EDS analysis, the grinding time was fixed at 3 h to cause a significant weight loss. The element content of the corroded coupon surfaces obtained at different pH values under different impressed currents was investigated by EDS. Figure 6 shows the EDS images of 1018 carbon steel after it was exposed to phosphate slurry at pH 3.1 with and without cathodic protection, respectively. Figure 6(Left) indicates that the atomic content was 39.71% for iron and 59.56% for oxygen. The stoichiometric ratio of Fe to O on the corroded surface of samples was 2:3, which suggests the formation of Fe_2O_3. After a polarization potential of −1.0 V was applied, the iron content reached 95.31% and oxygen content reduced to 4.38% as shown in Figure 6(Right). This indicates that the corroded surface was almost passivated when the polarization potential was applied. The impressed current cathodically polarized the coupon and reduced its

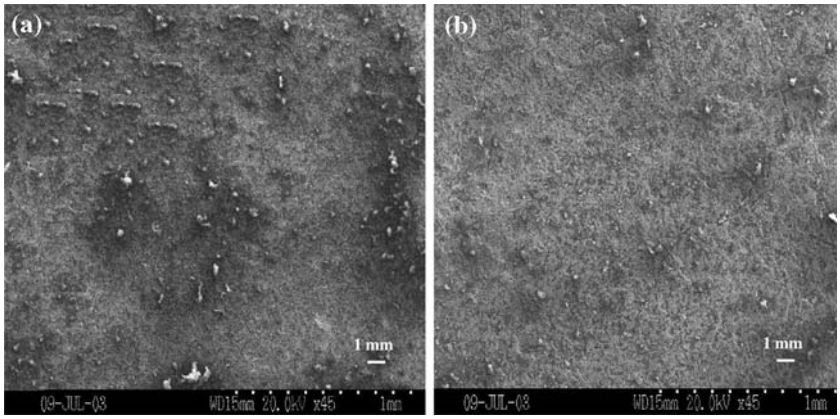

Fig. 5. SEM images of 1018 carbon steel exposed to phosphate slurry at pH 3.1 (a) without cathodic protection, (b) with polarization potential −1.0 V.

corrosion rate. Peng et al. [15] reached a similar conclusion from the study of the influence of high-energy krypton ions bombardment on the aqueous corrosion behavior of zirconium. The composition of the oxide film was determined by measuring the element ratio in the surface layer.

3.4.3. *XRD analysis*

The structure of the corrosion product of the coupons obtained after 3 h grinding at different pH values was investigated by X-ray spectrometer. Figure 7 shows the XRD patterns of 1018 carbon steel at pH 3.1 with and without cathodic protection, respectively. Figure 7(a) indicates that there existed iron (Fe) and ferric oxide (Fe_2O_3) on the coupon surface without cathodic protection. This suggests that Fe_2O_3 was the main corrosion product in the pH 3.1 solution [16]. Figure 7(b) shows the XRD patterns when a polarization potential of −1.0 V was applied. This figure reveals that corrosion was considerably reduced since Fe_2O_3 disappeared from the coupon surface. This conclusion is in good agreement with the Eh-pH diagram of Fe–O–H system [17], which indicates that Fe^{2+} and Fe_2O_3 were the most stable phases in the pH 3.1 solution without polarization potential, while Fe was the most stable phase when the −1.0 V polarization potential was applied to the metal surface. Many investigators [18–20] studied the surface properties of Fe, Fe_2O_3, and Fe_3O_4 films formed under different conditions. The characteristic peaks of Fe and Fe_2O_3 obtained from this study are consistent with these studies.

Similar results were obtained with 1018 carbon steel in the pH 6.8 and pH 9.2 solutions. The corrosion products were ferric oxide (Fe_2O_3), magnetite (Fe_3O_4) and ferric hydroxide ($Fe(OH)_3$) in the pH 6.8 solution and pH 9.2 solution [21, 22].

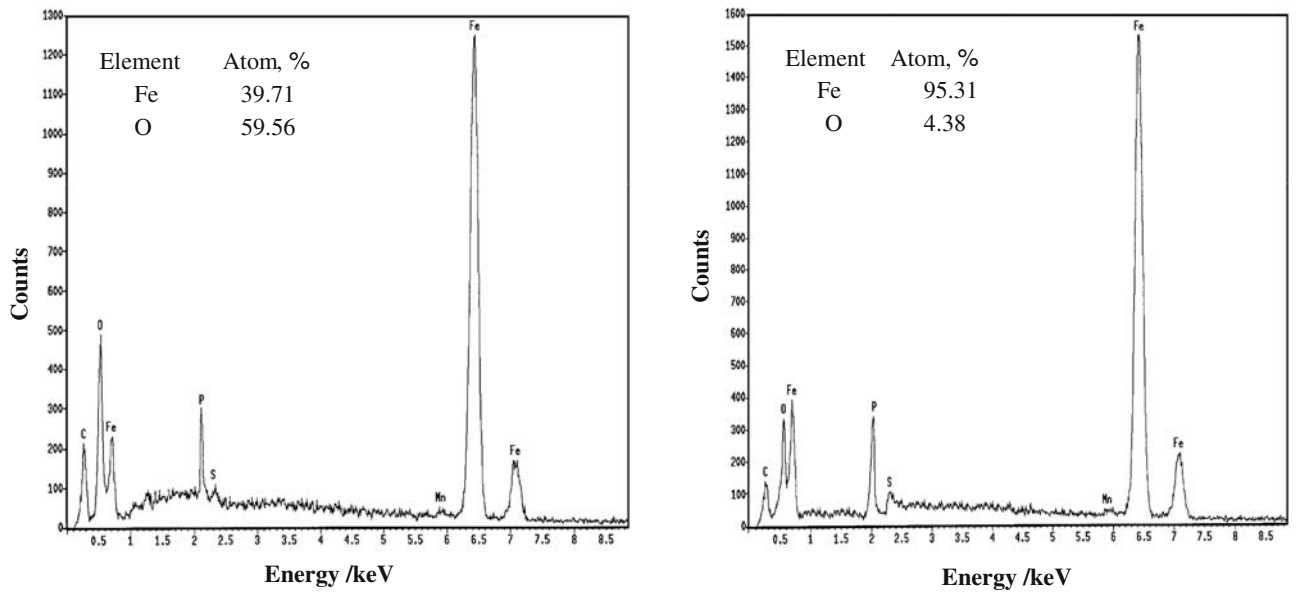

Fig. 6. EDS images of 1018 carbon steel exposed to phosphate slurry at pH 3.1 (Left) without cathodic protection, and (Right) with −1.0 V polarization potential.

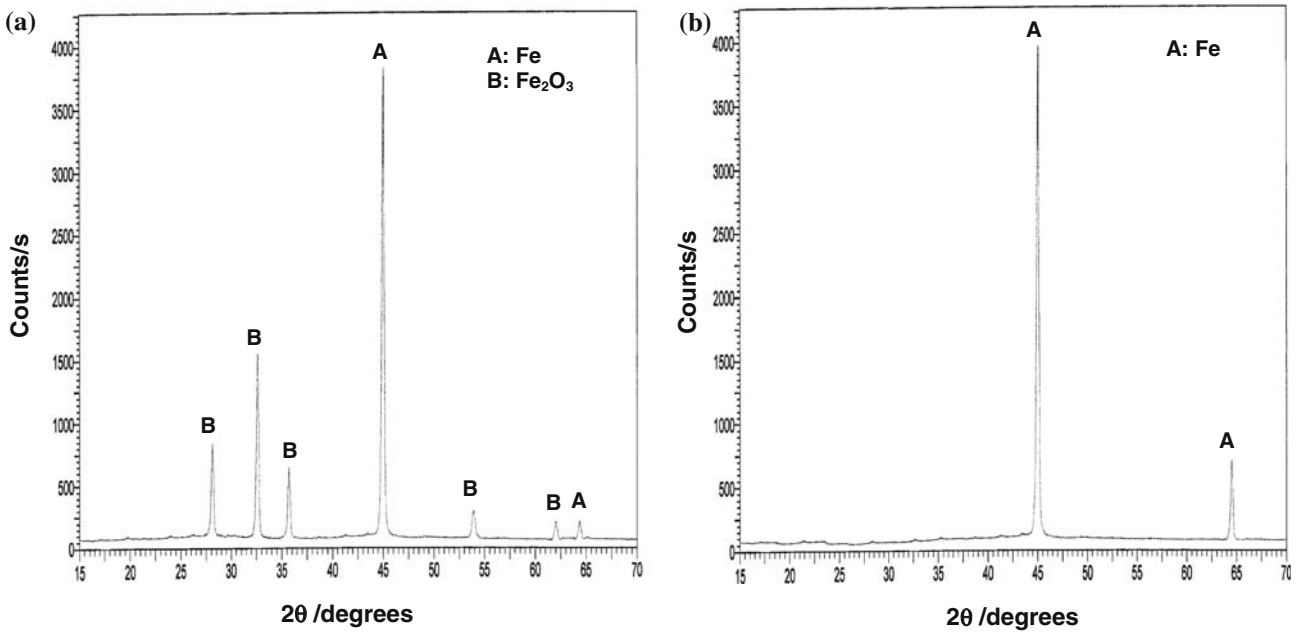

Fig. 7. XRD patterns of 1018 carbon steel exposed to phosphate slurry at pH 3.1 (a) without cathodic protection, and (b) with polarization potential −1.0 V.

4. Conclusions

Based on the above results, the following conclusions can be drawn:

(1) Polarization diagrams indicated that the current density was higher in nitrogenated solutions than in oxygenated solutions at the same pH value.
(2) Polarization potential of −1.0 V was sufficient to effectively reduce the wear rate of 1018 carbon steel. The total wear rate was reduced by 42% to 46% and corrosive wear rate was reduced by 84% to 86% when a potential of −1.0 V was applied at pH's of 3.1 to 9.2.
(3) The required current density to effectively reduce the wear rate of 1018 carbon steel was 210 mA m^{-2} in the pH 3.1 solution, 180 mA m^{-2} in the pH 6.8 solution, and 160 mA m^{-2} in the pH 9.2 solution.
(4) SEM analysis indicated that pitting corrosion was the main corrosion mechanism. SEM micro photographs suggested that corrosion was significantly reduced after a polarization potential of −1.0 V was applied.
(5) XRD patterns suggested that Fe_2O_3 was the main corrosion product for 1018 carbon steel in the pH 3.1 solution without cathodic protection, while Fe_2O_3, Fe_3O_4 and $Fe(OH)_3$ were the corrosion products in the pH 6.8 and pH 9.2 solutions.

Acknowledgement

The authors acknowledge the financial support from the Florida Industry of Phosphate Research (FIPR) under the grant number 00–01–170, which made this work possible.

References

1. J.J. Bartels and T.M. Gurr, in D.D. Carr (ed.), 'Phosphate rock, Industrial Minerals and Rocks', 6th edn. (SME, Littleton, Colorado, 1994), pp. 751.
2. P. Harben, *Industrial Minerals* **148** (1980) 48.
3. M.P. Allen, in H. El-Shall, B.M. Moudgil and R. Wiegel (Eds), The Vernal Phosphate Rock Mill, Beneficiation of Phosphate: Theory and Practice, (SME, Littleton, Colorado, 1993), pp. 85.
4. V. Shishodia, S. Rastogi and B. Pitchumani, in H. El-Shall, B.M. Moudgil and R. Wiegel (eds), Effect of Ball Size Distribution on Rock Phosphate Grinding in Industrial Ball Mill, Beneficiation of Phosphate: Theory and Practice, (SME, Littleton, Colorado, 1993), p. 157.
5. D.A. Jones, Principles and Prevention of Corrosion, 2nd edn. (1996) pp. 3–31.
6. D. Kotlyar, C.H. Pitt and M.E. Wadsworth, *Corrosion-NACE* **44**(4) (1987) 221.
7. R.L. Pozzo and I. Iwasaki, *J. Electrochem. Soc.* **136**(6) (1989) 1734.
8. R. Pazhianur, G.T. Adel, R.H. Yoon and P.E. Richardson, *Miner. Metall. Process.* **11** (1997) 1.
9. P.S. Liu, K.M. Liang and S.R. Gu, *Corros. Sci.* **43**(7) (2001) 1217.
10. M. Stern, *J. Electrochem. Soc.* **102** (1955) 609.
11. D. Tao, G.L. Chen and B.K. Parekh, *Corrosion* **60**(11) (2004) 1072.
12. D. Tao, G.L. Chen and B.K. Parekh, *Miner. Eng.* **18**(5) (2005) 481.
13. C.O. Emenike, *Anti-Corros. Methods Mater.* **42**(4) (1995) 6.
14. P.O. Gartland, R. Strommen and E. Bardal, *Mater. Perform.* **22**(6) (1983) 40.
15. D.Q. Peng, X.D. Bai, X.W. Chen, Q.G. Zhou, X.Y. Liu and R.H. Yu, *Appl. Surf. Sci.* **227** (2004) 73.
16. X. Wu and S.B. Kim, *Electrochem. Solid-State Lett.* **2**(4) (1999) 184.

17. J.R. Davis, Corrosion: Understanding the Basics, (ASM International, Materials Park, Ohio, 2000), pp. 1–377.
18. Y. Liu, W. Zhu, O.K. Tan and Y. Shen, *Mater. Sci. Technol.* **B4** (1997) 171.
19. H.Y. Zhang, J. Chen, Y.Y. He, X.M. Xue and S.Q. Peng, *Mater. Chem. Phys.* **55** (1998) 167.
20. R.N. Panda, N.S. Gajbhiye and G. Balaji, *J. Alloys Compd.* **326** (2001) 50.
21. G.B. Shan, H.Z. Liu, J.M. Xing, G.D. Zhang, Z.Y. Ma, X.Q. Liu and J.G. Liu, Surface Modification of Nano-magnetic Fe_3O_4 Particles and its Applications, EU Forum on Nanosized Technology, (Beijing, China, 2002), pp. 68.
22. B.C. Raymahashay and A.S. Khare, *Curr. Sci.* **84**(8) (2003) 1102.